

Electronic structure and relaxed geometry of the TiO₂ rutile (110) surface

D. Vogtenhuber, R. Podloucky, and A. Neckel

Institute of Physical Chemistry, Währingerstrasse 42, A-1090 Vienna, Austria

S. G. Steinemann

Institute de Physique Experimentale, Université de Lausanne, CH-1015, Dorigny-Lausanne, Switzerland

A. J. Freeman

Department of Physics and Astronomy, Northwestern University, Evanston, Illinois 60208

(Received 30 June 1993)

The *ab initio* full-potential linearized-augmented-plane-wave method for a free-slab geometry was used to calculate the electronic structure and geometry of a clean TiO₂ (110) rutile surface. Surface induced states were found in the density of states, such as an *s*-like surface state at -15 eV. Band bending states of width 0.5 eV appear just below the Fermi energy, in agreement with photoemission experiments. The positions of the atoms in the surface and subsurface layers and the corresponding change of Ti-O bond lengths were derived by total-energy minimization. In general, downward relaxations were obtained for which the fivefold-coordinated Ti experienced the largest relaxation of -0.180 Å, whereas the second most important relaxation effect, -0.156 Å, occurred for the surface O. The calculated Ti-O bond lengths are in very good agreement with experimental data for the TiO₂ (100) surface. The calculated work function 6.79 eV compares favorably with the experimental result of 6.83 eV. Based on an extension of density-functional theory to excited states the valence- and conduction-band gap was calculated to be 1.99 eV, which is in reasonable agreement with the experimental gap of 2.6 eV when compared to the one-particle band gap of 0.65 eV.

I. INTRODUCTION

TiO₂ surfaces have attracted increasing interest due to their properties for important applications such as the electrochemical photolysis of water¹ and as a support material for catalysts.² Ti-based alloys, as are used for bone and teeth implants, form oxide layers in aqueous solutions which, in combination with dissociated water molecules, function as the interface for the strong attachment of bone tissue.³ To describe and understand this type of interaction from first principles (as far as is possible at present), we apply the slab version of the full-potential linearized-augmented-plane-wave (FLAPW) method⁴ for the study of the clean and hydroxylized TiO₂ rutile surface. Our preliminary results on H and OH adsorption,^{5,6} in combination with ongoing improvements of code and algorithms, indicate that such a study is feasible with modern high-performance computers. Until the submission of our paper, no up-to-date first-principles calculation for the electronic structure and geometry optimization were available. Older electronic structure calculations were done with a linearized muffin-tin-orbital (LMTO) supercell approach⁸ and by a tight-binding scheme.⁹ When revising our paper, we were informed about extensive pseudopotential calculations on the same subject.⁷ The present paper comprises some of our most important results for the electronic structure and relaxed geometry for a clean TiO₂ rutile (110) surface. The rutile (110) surface was chosen because it is the most stable single-crystal surface for TiO₂ (Ref. 10) and, in addition, has rather high symmetry which facilitates the calcula-

tion. Geometry optimization is of particular importance for the study of adsorption processes, which will be our aim in the near future.

II. COMPUTATIONAL DETAILS

The electronic structure and total energy were calculated by the self-consistent FLAPW method⁴ within the local-density approximation (LDA) to density-functional theory. In particular, the LDA exchange-correlation potential and energy of Hedin and Lundqvist¹¹ was applied. During the self-consistency cycle and for geometry relaxation, four special two-dimensional \mathbf{k} points were taken for the valence states, whereas one two-dimensional \mathbf{k} point was chosen for a separate energy window to include Ti 3*s*- and 3*p*-like states. The plane-wave expansion of density and potential was cut off at 7.5 a.u.⁻¹, and the number of basis functions was restricted by a maximum momentum of 3.6 a.u.⁻¹, resulting in ≈ 1300 basis functions. Inside the muffin-tin spheres, density, potential, and basis functions were expanded up to $l=8$. The self-consistent potential was taken to calculate the density of states (DOS) for a grid of 12 \mathbf{k} points.

For the modeling of the rutile TiO₂ (110) surface, we constructed a free slab of total composition Ti₆O₁₂, consisting of three stoichiometric repeat units as (for positive z) shown in Fig. 1. The coordinate system of the slab is referenced to the central plane, which is the mirror plane of the slab. The corresponding bulk unit cell is shown by the dashed lines in Fig. 1. If the geometry is relaxed for the surface atoms, the corresponding positions are

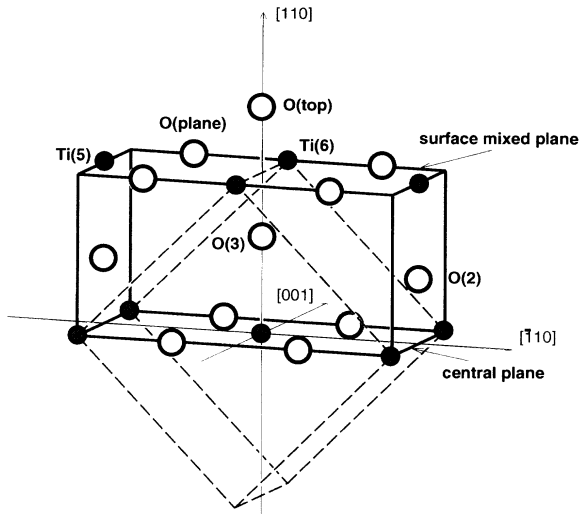


FIG. 1. Upper half of a TiO_2 (110) slab as used for the calculation. O atoms, empty spheres; Ti atoms, filled spheres. The rutile bulk unit cell is marked by dashed lines.

changed, and the mixed plane is deformed. This arrangement of atoms produces two distinctly different Ti positions concerning their nearest-neighbor oxygen environment: a sixfold-coordinated Ti, Ti (sixfold), as in the bulk, and a fivefold-coordinated Ti, Ti (fivefold), which is missing one oxygen due to the formation of the surface. The two-dimensional lattice parameters of the corresponding rectangular lattice are taken as $a = 6.495 \text{ \AA}$ and $b = 2.958 \text{ \AA}$.

III. ELECTRONIC STRUCTURE

The total DOS, total Ti, and local, layer decomposed DOS for O muffin-tin spheres are shown in Fig. 2 for the relaxed geometry. The states above E_F are shifted according to the gap correction discussed later. When discussing surface-induced features of the DOS, we refer to the local DOS of the surface O atom, O(top) (third panel in Fig. 2). The main features of the total DOS below E_F consist of an O s -like structure of width 2.5 eV around -18 eV separated by an intrinsic gap of 10 eV from the O p -like DOS of width 7 eV. The total DOS is analyzed by the predominant l -like components of the charge densities inside the muffin-tin spheres. A strikingly sharp peak is split away from the s -like DOS by about 1 eV which is associated with O(top), the surface O atom on top of the slab. This feature is basically caused by a positive shift of the Coulomb potential due to the missing stabilizing Ti neighbors. Although the s -peak of O(top) is very deep down in energy, it is a very sensitive indicator of adsorption processes, especially when the Coulomb potential of the surface O is strongly influenced by the adsorbed species [as, e.g., for H (Ref. 5)]. The DOS of the O atoms in the plane below the surface [see panel labeled O (plane)] coincides rather well in energy and in width with the DOS of the central layer of the film [panel O(center)]. The central layer is a mixed layer consisting

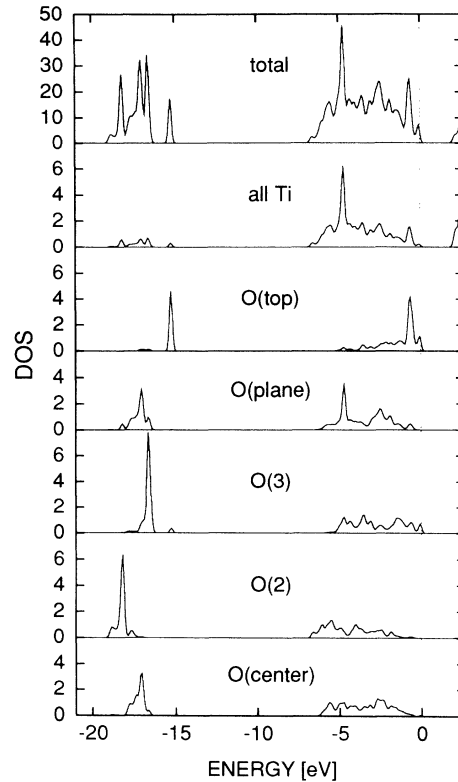


FIG. 2. Total density of states (states/eV), local Ti-DOS (sum over all Ti spheres in the unit cell), and layer-dependent local O-DOS (per O sphere). Atoms O(2) and O(center) belong to the central repeat unit. All other positions are indicated in Fig. 1.

of two Ti and two O atoms, whereas the surface plane containing O(plane) is warped by relaxation effects. Concerning only these specific DOS features, geometry relaxation is not significant. A small surface-induced DOS at -16 eV is found for O(3) which lies directly below O(top) (see Fig. 1). In general, the s -like features of O atoms sticking out of the planes such as O(2), O(3), and, in particular, O(top) are rather narrow and are remarkably shifted in energy in comparison to the DOS of O atoms in the planes. There is also a significant negative shift for the DOS of O(2) which is placed just above the central plane. Because the s -like bandwidth is rather narrow with respect to the energy shifts, these s -like peaks are even distinguished in the total DOS. The four sharp peaks of the total DOS can be ascribed (in ascending order according to Fig. 2) to O(2), O(3), the O atoms in the planes, and O(top). These peaks correspond to the layer-dependent shifts of the potentials, as is also reflected by the shifts of the O $1s$ levels relative to O(center), namely, -1.64 eV , $+0.72 \text{ eV}$, -0.11 eV , and $+1.18 \text{ eV}$ for the relaxed geometry, respectively. The corresponding $1s$ splits for the unrelaxed geometry are -1.58 eV , $+0.41 \text{ eV}$, -0.85 eV , and $+0.94 \text{ eV}$, correspondingly, showing that relaxation does not substantially change the oscillating behavior. Only O(plane) is more strongly affected by relaxation. The free slab we have studied does not have completely healed-out bulklike potentials, as can be seen from the splitting of 0.87 eV (relaxed) and 0.67 eV (unre-

laxed) of the Ti 3*p* levels in the central layer. The finiteness of our slab will influence the electronic structure to some extent. Characteristic surface features are also generated by the *p*-like DOS stretching from E_F down to about -7 eV. The DOS of O(top) is shifted towards less negative energies, producing a pronounced peak at -1 eV and some structure of width 0.5 eV just below E_F . This particular surface feature extends the bulklike DOS (as represented by the central layer DOS) up to E_F . Such surface-induced shifting of the top of the valence bands can be derived from the photoemission experiments of Kurtz *et al.*,¹² who observed a gap reduction of 0.4 eV when surface O defects were healed out. They discussed this result in terms of band bending of surface states. A remarkable peak of the total *p*-like DOS at -5 eV is attributed to the O(plane) DOS. There is also a remarkable Ti contribution [mainly consisting of Ti (fivefold) states] at this energy (see panel two in Fig. 2), which indicates the importance of the O(plane)-Ti(fivefold) interaction. As can also be seen from the total Ti-DOS, there is an appreciable amount of Ti 3*d* and O 2*p* hybridization.

Since we applied a free slab model with proper vacuum boundary conditions, we are able to define the work function correctly as the difference of the vacuum potential at (numerical) infinity and E_F . For the relaxed surface, we obtained 6.79 eV, which is in good agreement with the experimental result of 6.83 eV (Ref. 13) based on scanning tunneling microscopy data. According to our calculation, relaxation increases the work function by 0.13 eV.

IV. OPTIMIZED GEOMETRY

By minimizing the total energy, the positions of the top oxygen, O(top) and the atoms in the mixed bulk plane below, Ti(sixfold), Ti(fivefold), O(plane) were fully relaxed, preserving the symmetry of the two-dimensional unit cell derived from the bulk terminated (110) surface. The results are listed in Table I. All other positions deeper down in the slab were kept fixed.

It is known from experiment¹⁴⁻¹⁷ that under normal conditions the (110) surface does not reconstruct within experimental resolution. The strongest effect is obtained for Ti(fivefold) which sinks down by about 14%, in comparison to the bulk *z* position, towards the nearest oxygen inside the slab because the counterpart of this particular oxygen is missing due to the formation of the surface. Because of its sinking motion, the Ti(fivefold) drags with

TABLE I. Geometry changes (in Å) of surface and subsurface atoms of TiO₂ (110) relative to the unrelaxed surface mixed plane shown in Fig. 1. Bulk lattice parameters are $a = c = 6.495$ Å, $b = 2.958$ Å.

Atom	Bulk position			Relaxation	
	<i>x</i>	<i>y</i>	<i>z</i>	$\Delta(x,y)$	$\Delta(z)$
O(top)	0.000	0.000	1.267		-0.156
Ti(sixfold)	0.000	± 1.479	0		-0.049
Ti(fivefold)	± 3.248	0.000	0		-0.180
O(plane)	± 1.981	± 1.479	0	± 0.072	-0.115
O(3)	0.000	0.000	-1.267		kept fixed

it the four oxygens which originally were situated in the same mixed bulk plane. These O atoms were pulled down by about 9% and also moved in the *x* direction by about 4% towards the Ti(fivefold) atom. In our model they are free to move accordingly in the *x* direction without distorting the unit cell.

Because of the general downward movement, Ti(sixfold) also follows this trend although to a lesser degree than the fivefold coordinate Ti. The O(top) atom sticking out of the surface is pulled towards Ti(sixfold) (which is the nearest Ti neighbor) by about 8%. This particular Ti-O bond length is rather independent of the position changes of other surface atoms, indicating the locality inserted at least of this particular Ti-O bond. All these changes modify the Ti-O bonds lengths with respect to bulk distances, as summarized in Fig. 3. The bond lengths are generally reduced with the exception of the Ti(sixfold)-O(plane) length because the O atoms move away from this Ti atom towards Ti(fivefold), which tries to compensate in some way for the reduced local O coordination. Our calculated results appear to be in very good agreement with average Ti-O bond length changes obtained experimentally for the TiO₂ (100) surface by Zschack, Cohen, and Chung¹⁸ also showing reduced lengths in general. The (100) surface consists of pure

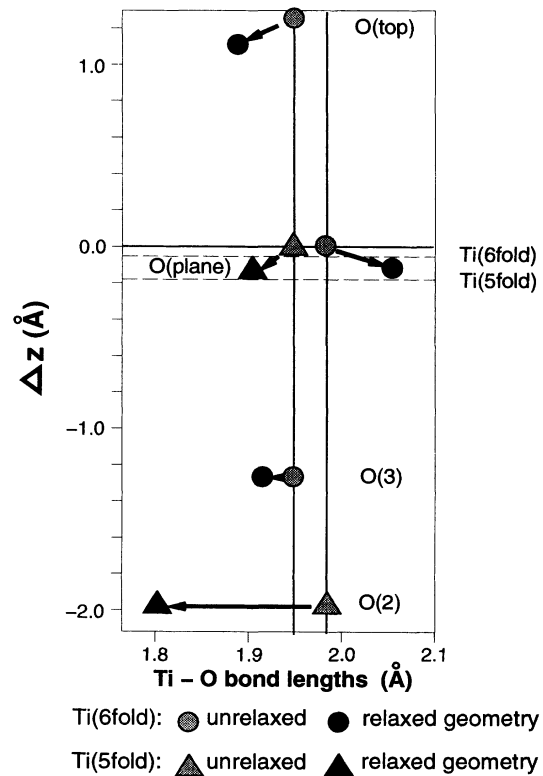


FIG. 3. Changes of nearest-neighbor Ti-O bond lengths vs *z*-position changes Δz with respect to the unrelaxed surface. Δz values of Ti atoms are indicated by dashed horizontal lines, the two different Ti-O bulk bond lengths of 1.947 Å and 1.981 Å are indicated by vertical lines. Ti(sixfold)-O bond lengths, circles; Ti(fivefold)-O bond lengths, triangles.

planes of Ti and O atoms and according to Zschack, Cohen, and Chung,¹⁸ reconstructs by the formation of a 1×3 geometry containing (110) microfacets. They conclude that only Ti atoms on the surface of the microfacets change their positions significantly. In the case of the (110) surface, rows of O are on top with a mixed Ti_2O_2 layer below which has two types of Ti at the surface. Zschack, Cohen, and Chung found the strongest Ti-O distance reduction for the top layer in very good agreement with our result for the bond length change between Ti(fivefold) and the bulklike O rows below the mixed plane. We calculated a stretching of the bond length that connects O(plane) and Ti(sixfold). The stretching is caused by the movement of these four O atoms towards Ti(fivefold). Again for the (100) surface, Zschack, Cohen, and Chung obtained a very similar stretched average bond length for the second and fifth layers, whereas for the third layer they derived an even stronger stretching. We have fully relaxed the top layer, namely, the surface layer consisting of O(top) rows of atoms and the layer consisting of atoms in the mixed plane. Further, but certainly much weaker relaxations could occur for deeper layers, which we did not calculate because of the finiteness of our slab. We expect that such secondary relaxations do not influence significantly our results because (within a simplified model) bonds seem to be rather localized as discussed above for the Ti(sixfold)-O(top) bond length. Furthermore, our results compare favorably with experimental data.¹⁸

Ramamoorthy, King-Smith, and Vanderbilt calculated, using a soft pseudopotential, the relaxations of the surface of a five-layer repeated slab, whereas we used a three-layer free slab and full-potential description. While we find inward relaxations of the top O and all the atoms in the mixed plane and, furthermore, lateral relaxation of O(plane), these authors report on (less pronounced) inward relaxation of O(top) and Ti(fivefold), but outward relaxation of O(plane) (without any move in the x direction) and Ti(sixfold). While the bond lengths of both calculations of the Ti(sixfold)-O(top) bond differ only by 0.2%, a net outward move of this group of atoms occurs in the pseudopotential calculation, in contrast to our results. Furthermore, we find a stronger compensation of the loss of coordination of Ti(fivefold), caused by a general reduction of the remaining Ti(fivefold)-O bond lengths, while Ramamoorthy, King-Smith, and Vanderbilt report on a much lesser decrease of the Ti(fivefold)-O(2) distance and even an increase of the Ti(fivefold)-O(plane) bond length.

V. GAP CORRECTION

An important physical property of insulating materials is the size of the band gap between valence- and conduction-band states. Usually, the gaps derived from the Kohn-Sham equations are substantially smaller than experimental values because density-functional theory (DFT) in its original formulation by Hohenberg, Kohn, and Sham^{19,20} is only meaningful for ground state properties such as the total energy and the charge density. If one wants to calculate correctly gaps originating from

transitions of valence-band electrons to conduction-band states, one has to extend the original DFT to excited states.

Within DFT, the band gap can be defined by the difference of ground-state total energies of the N and $(N + 1)$ electron systems.²¹ Such an approach is, however, not easily applicable. Several authors^{21–24} have worked on the discontinuity in the exchange-correlation potential which occurs during the passage from an (N) to an $(N + 1)$ -particle system; this gives rise to a contribution to the band gap which is of the same order of magnitude as the difference of the corresponding Kohn-Sham eigenvalues. To accommodate this effect, the scissors operator was introduced, which causes a constant energy shift of the energy levels of the states in the conduction band.

For calculation of the band gap of TiO_2 (110) we applied the more general approach of Fritsche's generalized density-functional (GDF) theory.^{25,26,29} As distinguished from calculations that directly focus on the difference between quasiparticle energies,^{21,23,24} Fritsche²⁵ derived an alternative expression by considering the difference of the corresponding total energies. The band-gap correction to the Kohn-Sham eigenvalues difference Δ ,

$$E_{\text{gap}} = \varepsilon_f - \varepsilon_i + \Delta, \quad (1)$$

defined by

$$\Delta = \int [|\psi_f(\mathbf{r})|^2 - |\psi_i(\mathbf{r})|^2][2\bar{\varepsilon}_{\text{xc}}^{(0)}(\mathbf{r}) - V_{\text{xc}}^{(0)}(\mathbf{r})]d\mathbf{r}, \quad (2)$$

acts like the scissors operator. In Eq. (1), ε_i and ε_f denote, respectively, the eigenvalue of the highest occupied valence-band (or initial) state ψ_i and the eigenvalue of the lowest unoccupied conduction-band (or final) state ψ_f of the Kohn-Sham equation. Because we consider the LDA to be a good approximation in the case of TiO_2 , we took the corresponding LDA expressions of Hedin and Lundqvist¹¹ for the exchange-correlation energy per particle $\bar{\varepsilon}_{\text{xc}}^{(0)}$ and for the exchange-correlation potential $V_{\text{xc}}^{(0)}(\mathbf{r})$ that we used for all of our results. With that assumption, Δ can be calculated easily. It should be noted that the band-gap correction describes itinerant excitations for which Hartree terms due to charge-transfer effects cancel out.^{26,28} The gap corrections as we applied in our study work well for systems with substantially different gap sizes.²⁹

The energy regime of the occupied states close to E_F is dominated by O(top)- p -like surface states. Utilizing a grid of 12 \mathbf{k} points for the DOS calculation, the highest occupied state is found for $\mathbf{k} = (\frac{1}{8}, \frac{1}{8})$, the lowest conduction-band state (which is of Ti- d -like character, as also can be seen from panel two in Fig. 2) is obtained for $\mathbf{k} = (0, 0)$. The difference between the Kohn-Sham energies of these two states amounts to 0.65 eV, which, as expected, is substantially smaller than the experimental value of 2.6 eV.¹² However, the correction ($\Delta = 1.34$ eV), is twice as large as the eigenvalue differences, and gives the main contribution to E_{gap} . The final value for E_{gap} is thus 1.99 eV and agrees very well with the calculation of Ref. 27, where a compete-neglect-of-differential-overlap-like method with parameters fitted to reproduce experi-

mental bulk properties was used. Although this value is still smaller than the experimental value of 2.6 eV,¹² the band-gap correction can be considered to work reasonably well because it leads to a substantial improvement. Ramamoorthy, King-Smith, and Vanderbilt find a direct gap of 2 eV without any gap correction at the point Γ . Fritsche and Gu²⁹ obtained very good results (as compared to experiment) for large gap bulk insulators for which the gap correction was as large as the Kohn-Sham difference. They also took into account nonlocal corrections to the LDA, which, however, appeared to be insignificant.

VI. SUMMARY

In conclusion, the FLAPW *ab initio* approach yields results which are consistent with the available experimental information for the electronic structure as well as for the relaxed geometry of the clean TiO₂ rutile (110) surface. We therefore believe that such an approach is also

able to treat the very important problem of chemisorption of small molecules (such as water) on oxides surfaces (such as TiO₂), which is our next goal.

ACKNOWLEDGMENTS

This work was supported by the Austrian Fonds zur Förderung der wissenschaftlichen Forschung (Projekt No. P8708) and by the Austrian Bundesministerium für Wissenschaft und Forschung (GZ.49.731/2-24/91), by the Swiss foundation "Herbette Stiftung" at Univ. Lausanne, by the Swiss National Science Foundation (Projekt No. 20-31191.91), and by the U.S. Department of Energy (Grant No. DE-FG02-88ER 45372). Most of the calculations were performed on the NEC-SX3 of CSCS (Manno, Switzerland), and part of the computations were done on the CRAY2 of SIC at the EPFL (Lausanne, Switzerland). Also, the support of the Computing Center of the University of Vienna is gratefully acknowledged.

¹A. Fujishima and K. Honda, *Nature* **238**, 37 (1972).

²J. P. Bucher, J. J. van der Klink, and M. Graetzel, *J. Phys. Chem.* **94**, 1209 (1990).

³S. G. Steinemann, in *Oral Implantology*, edited by A. Schroeder, F. Sutter, and G. Krekeler (Thieme Medical, New York, 1991), p. 37.

⁴H. Krakauer, M. Posternak, and A. J. Freeman, *Phys. Rev. B* **19**, 1706 (1979); M. Posternak, H. Krakauer, A. J. Freeman, and D. D. Koelling, *ibid.* **21**, 5601 (1980); E. Wimmer, H. Krakauer, M. Weinert, and A. J. Freeman, *ibid.* **24**, 864 (1981).

⁵R. Podloucky, S. G. Steinemann, and A. J. Freeman, *New J. Chem.* **16**, 1139 (1992).

⁶R. Podloucky, S.G. Steinemann, and A. J. Freeman, in *Tissue-inducing Biomaterials*, MRS Symposia Proceedings No. 252, edited by M. Flanagan, L. Cima, and E. Ron (Materials Research Society, Pittsburgh, 1992), p. 43.

⁷M. Ramamoorthy, R. D. King-Smith, and D. Vanderbilt (unpublished); we are grateful to D. Vanderbilt for sending us the unpublished manuscript.

⁸R. V. Kasowski and R. H. Tait, *Phys. Rev. B* **20**, 5168 (1979).

⁹S. Munnix and M. Schmeits, *Phys. Rev. B* **28**, 7342 (1983); **30**, 2202 (1984).

¹⁰V. E. Henrich, *Prog. Surf. Sci.* **14**, 175 (1983).

¹¹L. Hedin and S. Lundqvist, *J. Phys.* **33**, C3-73 (1972).

¹²R. L. Kurtz, R. Stockbauer, T. E. Madey, E. Román, and J. L. de Segovia, *Surf. Sci.* **218**, 178 (1989).

¹³R. Emch, Ph.D. thesis, University of Geneva, 1990.

¹⁴P. J. Møller and M.-C. Wu, *Surf. Sci.* **224**, 265 (1989).

¹⁵B. L. Maschoff, J.-M. Pan, and T. E. Madey, *Surf. Sci.* **259**, 190 (1991).

¹⁶A. E. Taverner, P. C. Hollamby, P. S. Aldridge, and R. G. Eg-dell, *Surf. Sci.* **287/288**, 653 (1993).

¹⁷R. Heise and R. Courths, *Surf. Sci.* **287/288**, 658 (1993).

¹⁸P. Zschack, J. B. Cohen, and Y. W. Chung, *Surf. Sci.* **262**, 395 (1992).

¹⁹P. Hohenberg and W. Kohn, *Phys. Rev.* **136**, B864 (1964).

²⁰W. Kohn and L. J. Sham, *Phys. Rev.* **140**, A1133 (1965).

²¹R. W. Godby, M. Schlüter, and L. J. Sham, *Phys. Rev. B* **37**, 10 159 (1988).

²²J. P. Perdew and M. Levy, *Phys. Rev. Lett.* **51**, 1884 (1983).

²³L. J. Sham and M. Schlüter, *Phys. Rev. Lett.* **51**, 1888 (1983).

²⁴L. J. Sham and M. Schlüter, *Phys. Rev. B* **32**, 3883 (1985).

²⁵L. Fritsche, *Phys. Rev. B* **33**, 3976 (1985).

²⁶L. Fritsche, *Physica B* **172**, 7-17 (1991).

²⁷C. Noguera, J. Goniakowski, and S. Bouette-Russo, *Surf. Sci.* **287/288**, 188 (1993).

²⁸L. Fritsche (private communication).

²⁹L. Fritsche and Y. M. Gu, *Phys. Rev. B* **48**, 4250 (1993).

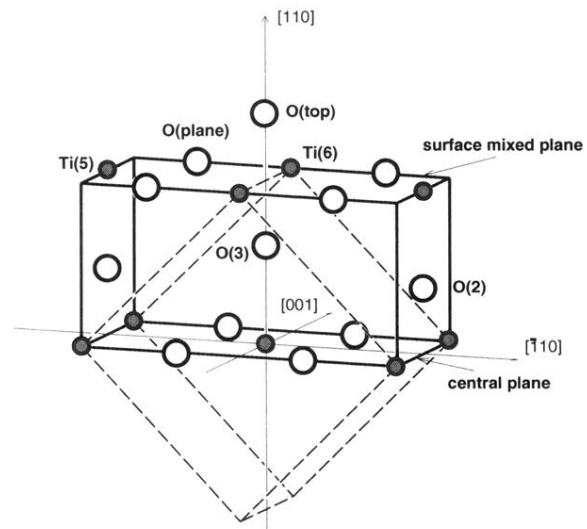


FIG. 1. Upper half of a TiO_2 (110) slab as used for the calculation. O atoms, empty spheres; Ti atoms, filled spheres. The rutile bulk unit cell is marked by dashed lines.

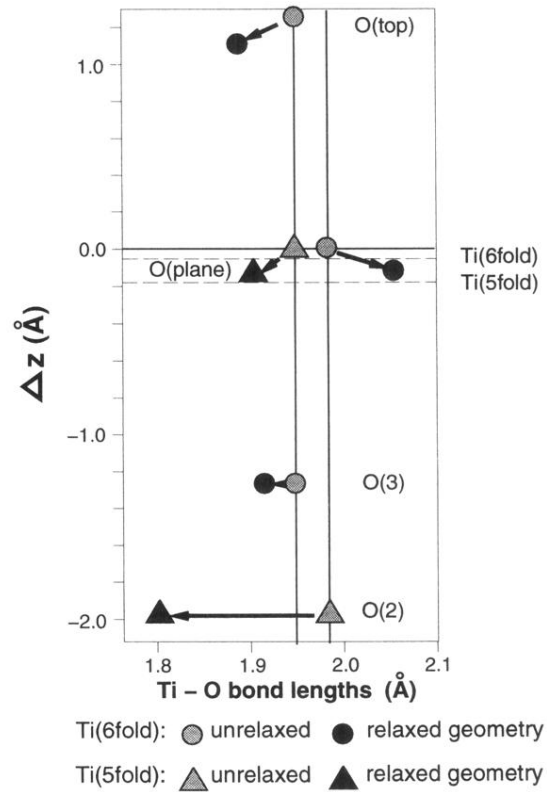


FIG. 3. Changes of nearest-neighbor Ti-O bond lengths vs z-position changes Δz with respect to the unrelaxed surface. Δz values of Ti atoms are indicated by dashed horizontal lines, the two different Ti-O bulk bond lengths of 1.947 Å and 1.981 Å are indicated by vertical lines. Ti(sixfold)-O bond lengths, circles; Ti(fivefold)-O bond lengths, triangles.